Dalton Transactions

Accepted Manuscript

This is an *Accepted Manuscript*, which has been through the Royal Society of Chemistry peer review process and has been accepted for publication.

Accepted Manuscripts are published online shortly after acceptance, before technical editing, formatting and proof reading. Using this free service, authors can make their results available to the community, in citable form, before we publish the edited article. We will replace this *Accepted Manuscript* with the edited and formatted *Advance Article* as soon as it is available.

You can find more information about *Accepted Manuscripts* in the Information for Authors.

Please note that technical editing may introduce minor changes to the text and/or graphics, which may alter content. The journal's standard Terms & Conditions and the Ethical guidelines still apply. In no event shall the Royal Society of Chemistry be held responsible for any errors or omissions in this *Accepted Manuscript* or any consequences arising from the use of any information it contains.

ROYAL SOCIETY OF CHEMISTRY

www.rsc.org/dalton

Synopsis (Graphic)

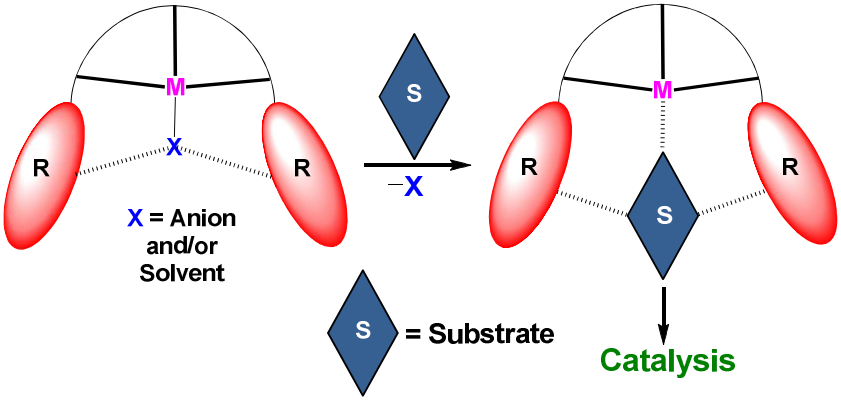

Synopsis (Abstract)

Coordination complexes of amide-based ligands with appended heterocyclic rings create a hydrogen bonding cavity that effectively bind the substrate(s). Such cavity-based complexes function as reusable and heterogeneous catalysts for the ring-opening reactions of epoxides; cyanation reactions of aldehydes; and epoxidation reactions of olefins.

Dalton Transactions Accepted Manuscript

Journal Name

RSCPublishing

ARTICLE

Mononuclear complexes of amide-based ligands containing appended functional groups: Role of secondary coordination sphere on catalysis

Deepak Bansal,[a] Gulshan Kumar,[a] Geeta Hundal[b] and Rajeev Gupta*[a]

Cite this: DOI: 10.1039/x0xx00000x

Received 00th January 2012,
Accepted 00th January 2012

DOI: 10.1039/x0xx00000x

www.rsc.org/

Amide-based ligands H_2L^1, H_2L^2 and H_2L^3 containing thiazole, thiazoline and benzothiazole appended groups have been used to synthesize Zn^{2+} (**1** and **3**), Cd^{2+} complexes (**2** and **4**); and a Mn^{2+} complex (**5**). In all cases, potentially multidentate ligands create a meridional N_3 coordination environment around the M(II) ion whereas additional sites are occupied by labile nitrate ion in **1** – **4** and MeOH in **5**. Interestingly, metal complexation caused the migration of protons from amidic N-H sites to the appended heterocyclic rings in complexes. Structural studies show that the protonated heterocyclic rings in all complexes create a hydrogen bond based cavity adjacent to metal ion. Importantly, binding studies confirm that the substrates are bound within the complex cavity closer to the Lewis acidic metal in all complexes including the oxidation-sensitive Mn ion in complex **5**. All complexes have been utilized as the reusable and heterogeneous catalysts for ring-opening reactions of assorted epoxides; cyanation reactions of various aldehydes; and epoxidation reactions of several olefins.

Introduction

In recent years, significant interest has been devoted to develop metal-based catalysts due of their uniqueness in controlling reactivity and selectivity of a transformation.[1] The motivation for such metal mediated catalytic transformations is derived from biological systems which are paramount for the precise control over the reactivity and selectivity.[2] Importantly, biological catalysts achieve such an extraordinary feat by the modulation of secondary coordination sphere and often create a substrate-specific cavity for the binding and activation of a substrate.[2] For secondary coordination sphere, hydrogen bonding (H-bonding) sensitive functional groups play crucial role in holding and organising the substrate closer to the metal site.[3] However, incorporation of desired secondary coordination sphere adjacent to a metal site is always a daunting challenge in synthetic complexes. Thus, continuous efforts are being made to enhance the catalytic relevance and performance of metal-based catalysts by incorporating functional groups capable of fostering weak interactions including hydrogen bonds (H-bonds).[4] Conceptually, scheme 1 explains our approach of cavity based catalyst where central part of a multidentate ligand coordinates a metal ion whereas appended "R" groups create an artificial cavity capable of interacting and organising the substrate "S" closer to the metal center. Such a situation is likely to enhance the interaction of substrate to metal ion and therefore may assist in its activation and subsequent transformation.

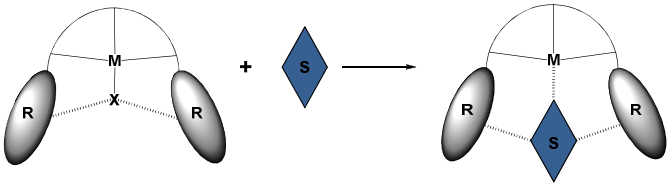

Scheme 1. Schematic representation for possible activation of substrate within the cavity as expected from complexes **1** – **5**. M = Metal: X = anion and/or solvent; R = Appended groups; S = Substrate.

In this context, multidentate ligands containing appended functional groups have shown promising results by showcasing creation of secondary coordination sphere adjacent to metal site.[5] Out of various multidentate ligands, ligands based on pyridine-2,6-dicarboxamide scaffold have displayed noteworthy results in recent time.[6,7] Such ligands[8] in their deprotonated form generate a pincer cavity via two *N*-amidate groups and an anchoring pyridine ring that strongly hold a metal ion while appended functional groups are adequately positioned to create secondary coordination sphere. Fiedler and co-workers[9] have used pyridine-2,6-dicaboxamide ligands appended with pyridine, pyrimidine or quinolone rings to prepare their Cu(II) complexes. Interestingly, protonation of the appended heterocyclic rings was observed during the synthesis and such rings create intramolecular H-bonds to the ligated chloro and/or aqua ligand. Wright and co-workers[10] have also used a similar ligand

Dalton Transactions Accepted Manuscript

to prepare a Ru(II) complex where protonated pyridine rings formed H-bonds to the ligated chloro ligand.

These examples nicely illustrate that the substituted pyridine-2,6-dicarboxamide-based ligands are attractive frameworks for the incorporation of second-sphere H-bonding interactions into the transition-metal complexes. In this work, we have used similar ligands based on pyridine-2,6-dicarboxamide scaffold; however, with assorted appended groups. We show that such appended functional groups in the resultant coordination complexes create an H-bonding based cavity around the metal ion. Our results suggest that the presence of cavity adjacent to metal ion assist in holding and organising the substrate closer to the catalytic site. In particular, ligands H_2L^1, H_2L^2 and H_2L^3 having thiazole, thiazoline and benzothiazole appended groups (Figures S1 – S9; ESI) have been used to synthesize Zn^{2+} (**1** and **3**) and Cd^{2+} complexes (**2** and **4**); and a Mn^{2+} complex (**5**) (Scheme 2). These well-characterized complexes have been used as the reusable and heterogeneous catalysts for the ring-opening reactions (RORs); cyanation reactions (CRs); and epoxidation reactions (ERs).

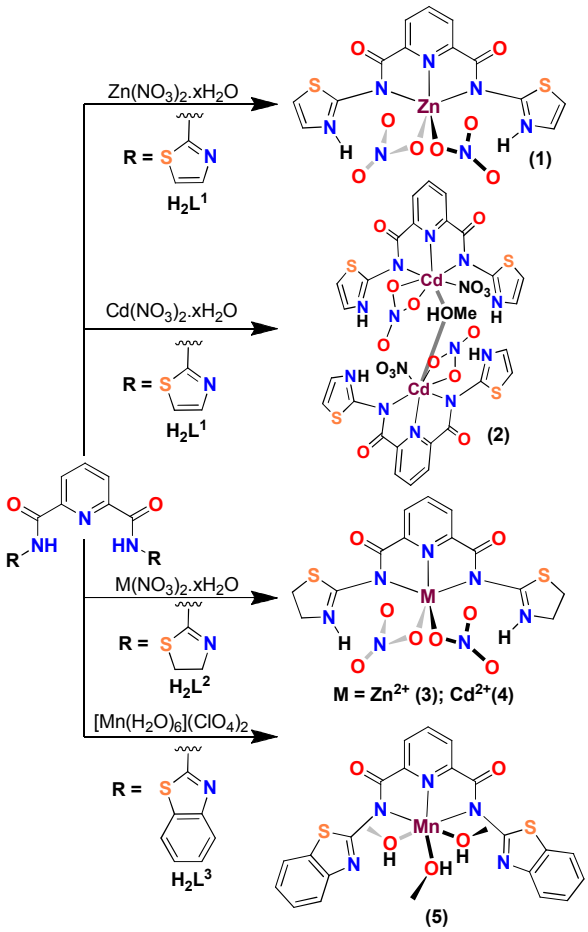

Scheme 2. Preparative routes for the synthesis of complexes **1-5**.

Results and Discussion

Synthesis and characterisation of complexes 1-5

This works discusses two types of coordination complexes; **1** – **4** that are based on Zn(II) and Cd(II) ions and **5** which is a Mn(II) complex. Complexes **1** – **4** were synthesised by treating ligand H_2L^1 or H_2L^2 with $[M(NO_3)_2].xH_2O$ without any requirement of a base. Interestingly, complexation resulted in the migration of protons from amidic N-H sites to the appended heterocyclic rings. Complex **5**, however, was synthesised by treating the deprotonated form of ligand H_2L^3 with $[Mn(H_2O)_6](ClO_4)_2$. All complexes were obtained as pale yellow crystalline material after standard workup and recrystallization. FTIR spectra of complexes **1**, **3** and **4** revealed an isostructural nature except for the minor differences due to different appended rings. The $\nu_{C=O}$ stretches for **1** – **4** were noted at 1612-1654 cm^{-1} which were red-shifted by 40–60 cm^{-1} than their respective ligands and suggest the involvement of deprotonated $N_{amidate}$ in bonding.[11] In addition, ν_{NH} stretches for the protonated heterocyclic rings appeared at 3276 and 3195 cm^{-1} for **1** and **2** while at 3323 and 3319 cm^{-1} for **3** and **4**, respectively. These N-H stretches are significantly different (ca. 85 – 160 cm^{-1}) when compared to the original ligands and conclusively prove that the protons have been re-located (Figures S10-S13, ESI). The presence of nitrate ion was established by the observation of $\nu_{N=O}$ stretches at 1335-1355, 1268-1287, and 1016-1027 cm^{-1}. Complex **5** exhibits ν_{O-Me} stretch at 1016 cm^{-1} indicative of coordinated methanol.[11] The conductivity measurements[12] substantiate that the nitrate ions in complexes **1** – **4** are loosely coordinated and are dissociated once these complexes are dissolved in DMF or DMSO. The absorption spectra of ligands H_2L^1, H_2L^2 and H_2L^3 exhibit λ_{max} at 303, 285 and 310 nm, respectively. Complexes **1**, **2** and **5** display bathochromically shifted λ_{max} at 325, 330 and 340 nm, respectively whereas complexes **3** and **4** exhibit spectral features below 300 nm (Figure S14, ESI). Complexes **1** – **4** have also been characterised by the ^1H NMR spectra and display minor changes in chemical environment when compared to free-ligand spectra (Figures S15 – S18, ESI). Notably, NMR spectra also established the presence of heterocyclic N-H protons that disappeared on deuterium exchange.

Crystal Structures

All five complexes; $[\{\mathbf{L}^1(H)_2\}Zn(NO_3)_2]$ (**1**), $[\{\mathbf{L}^1(H)_2\}Cd(NO_3)_{1.5}]_2$ (μ-OCH_3) (**2**), $[\{\mathbf{L}^2(H)_2\}Zn(NO_3)_2]$ (**3**), $[\{\mathbf{L}^2(H)_2\}Cd(NO_3)_2]$ (**4**) and $[Mn(L^3)(CH_3OH)_3]$ (**5**) have been crystallographically characterised. The molecular structures of complexes **1**, **2** and **5** are shown in figures 1, 2 and 3 whereas crystal structures of **3** and **4** are presented in figures S19 and S20. The selected bonding parameters are contained in Tables S1 and S2.

Dalton Transactions Accepted Manuscript

This journal is © The Royal Society of Chemistry 2012

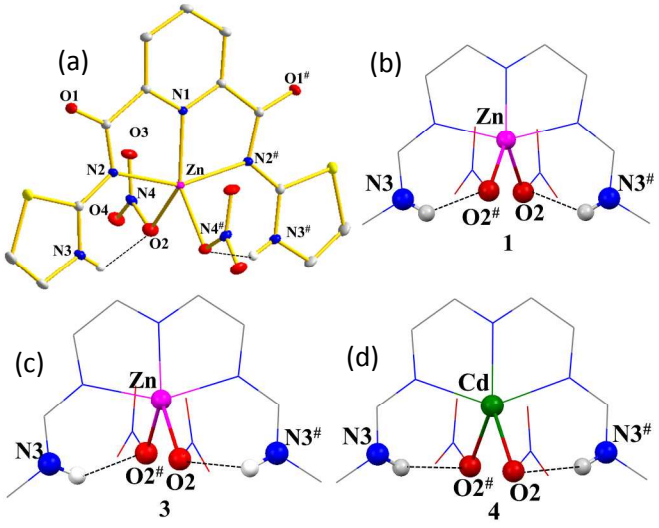

Figure 1. (a) Thermal ellipsoidal representation of complex **1**; ellipsoids are drawn at 30% probability level whereas only selected hydrogen atoms are shown for clarity. (b-d) Secondary coordination sphere created by the protonated heterocyclic rings around the nitrate ions in complexes **1**, **3**, and **4**.

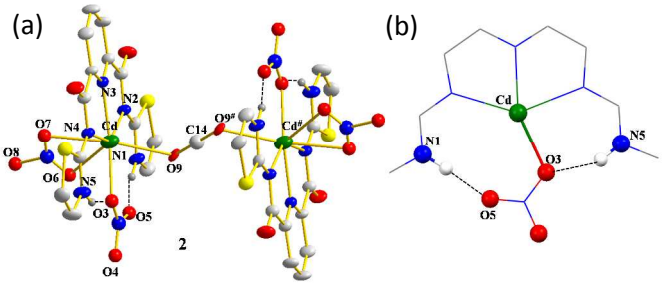

Figure 2. (a) Thermal ellipsoidal representation of complex **2**; ellipsoids are drawn at 30% probability level whereas only selected hydrogen atoms are shown for clarity. (b) Secondary coordination sphere created by the protonated heterocyclic rings around the nitrate ion in complex **2**.

Crystal Structures of 1, 3 and 4

The complexes **1**, **3** and **4** are isostructural; however with two different ligands. The crystal structures of these three complexes show that the metal ion is present in the pincer part of the ligand and is coordinated to two deprotonated N_{amide} groups and a $N_{pyridyl}$ atom. The M-N_{amide} bond lengths are longer than that of M-$N_{pyridyl}$ distances. In addition, two nitrate ions coordinate the metal center with highly asymmetrical M-$O_{nitrate}$ bond distances. The geometry around the metal in complexes **1, 3** and **4** can be described as distorted square-pyramidal (with monodentate nitrate) with a large τ_5 distortion parameter of 0.303 and 0.247 for complexes **1** and **3**, respectively.[13] The ideal value of τ_5 is 0 and 1 for a perfect square-pyramidal and trigonal-bipyramidal geometry.[13] Importantly, both appended heterocyclic rings in all three complexes are protonated due to the migration of protons from amidic N-H groups to these rings. The result is the generation of thiazolium and thiazolinium rings in these complexes. Such a protonation results in the formation of H – bonds from the protonated rings to the coordinated nitrate anions. The heterocycle-H…ONO_2 H-bonding synthons display O···N heteroatom separations between 2.869 – 2.995 Å. An interesting consequence of such H-bonding is the orientation of the coordinated nitrate anion within the complex cavity and may have noteworthy implications during the catalysis.

Crystal structure of 2†

The crystal structure of complex **2** is quite different from complexes **1**, **3** and **4** due to a dinuclear nature of complex and the presence of a bridging methoxide ion. Every Cd^{2+} ion displays a seven-coordinate geometry where ligand coordinates in a N_3 meridional fashion while one nitrate ion ligates in a bidentate η-1,2-mode and the second one is monodentate. Notably, two monomeric halves are bridged by a methoxide ion with Cd…OMe distance of 2.474 Å. The Cd…ONO_2 distances vary between 2.262 – 2.535 Å with monodentate nitrate ion making shorter bonds. In this case also, nitrogen atoms of the appended heterocyclic rings are protonated to afford thiazolium moieties. Such thiazolium rings are involved in H-bonding with the O atoms of monodentate nitrate ions. The heteroatom separations for the $O3_{nitrate}$…H5–N5 and $O5_{nitrate}$…H1–N1 synthons are 2.747 and 2.726 Å, respectively.

Crystal structure of 5

Complex **5** displays a similar structure to that of complexes **1**, **3**, and **4**; however, without protonation of the appended heterocyclic rings. Here Mn^{2+} ion is present in the pincer part of the ligand coordinated by two anionic N_{amide} and one neutral $N_{pyridyl}$ atoms while additionally ligated by three methanol molecules. The Mn-N_{amide} and Mn-$N_{pyridyl}$ bond lengths are comparable whereas Mn…O(H)Me distances vary between 2.128 – 2.205 Å. The geometry around the Mn^{2+} ion can be best described as distorted octahedral with two methanol molecules occupying the axial positions. Complex **5** displays reversed arrangement of H-bonding interactions than what observed in complexes **1** – **4**. In this case, appended heterocyclic rings function as the H-bond acceptors whereas coordinated methanol molecules serve as the H-bond donors. For heterocycle-N…H-OCH_3 synthon, the heteroatom separation is 2.653 Å.

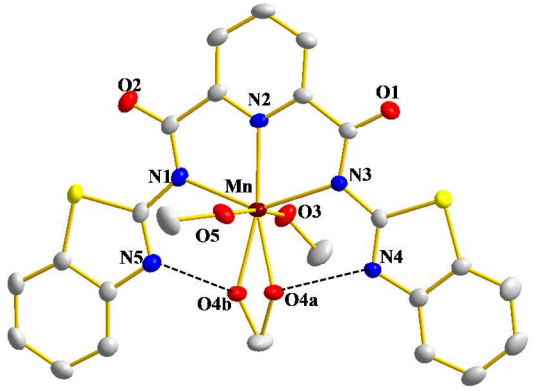

Figure 3. Thermal ellipsoidal representation of complex **5**; ellipsoids are drawn at 30% probability level whereas hydrogen atoms are omitted for clarity.

Dalton Transactions Accepted Manuscript

Except complex **2**, all other complexes display interesting solid-state packing due to the involvement of $O_{nitrate}$…H–N_{ring}, C–H…$O_{nitrate}$ and O_{amide}**…**H–O_{MeOH} intermolecular H-bonding interactions. In particular, complexes **1**, **3,** and **4** form zig-zag chains due to the operation of $O_{nitrate}$…H–N_{ring} H-bonding interactions whereas complex **5** generates a similar H-bonding motif due to the O_{amide}**…**H–O_{MeOH} intramolecular interactions (Figures S21 – S25 and Tables S3 – S7; ESI).

Lewis acidic catalytic applications

One of the objectives in this work was to evaluate the catalytic efficiency of the synthesized complexes. This was due to a notable cavity structure and the presence of intramolecular H-bonds in all five complexes. We envisioned that such structural features may assist in holding a substrate closer to the Lewis acidic metals in all five complexes including oxidation-sensitive Mn ion in complex **5**. For Lewis acidic-based catalysis, we selected ring-opening reactions (RORs) of epoxides and cyanation reactions (CRs) of aldehydes. RORs of epoxides with a variety of nucleophiles have attracted immense research due to the pharmaceutical and commercial importance of ring-opened products.[14] In such reactions, activation of epoxide-based substrate is a prerequisite for catalysis and assorted chemicals/reagents[15] including well-defined complexes[16] have been used for such an activation. Our complexes with Lewis acidic metals and weakly coordinated nitrates ions and/or labile MeOH molecules offered a perfect platform to explore RORs. We anticipated that the oxygen-based substrates are likely to replace labile nitrate ions[16b] and/or MeOH molecules and the complex cavity lined with H-bond sensitive functional groups may assist in directing the substrate towards the metal ion. We, therefore, believed that the cavity may play subtle yet decisive role in holding the substrate while the Lewis acidic metal activates the substrate before the attack of nucleophile. In order to minimize the competition from solvent molecules, we decided to use solvent-free reaction conditions for catalysis. Of course, such reactions provide notable advantages such as efficient separation of products, easy recovery of catalyst, non-interference of solvent molecules, and high conversion. For a typical aminolysis reaction, when cyclohexene oxide was stirred with only 2 mol% of complexes **1 – 5** followed by the addition of aniline, a smooth reaction took place that produced the corresponding *β*-amino alcohol in high yield. As shown in Table 1, all five catalysts were equally effective in promoting the reaction between cyclohexene oxide with aniline (entry 1) as well as with assorted *para*-substituted anilines containing electron-donating or electron-withdrawing functional groups (entries 2-5).

Table 1. Ring-opening reactions of cyclohexene oxide (1-5) and styrene oxide (6-10) with aniline and *para*-substituted anilines using complexes **1 – 5**.[a]

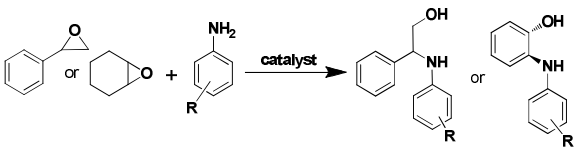

Entry	R	%Yield[b]				
		1	**2**	**3**	**4**	**5**
1	-H	97, 95[c], 94[d]	97, 96[c], 94[d]	98	98	94
2	-C_2H_5	92	89	93	90	92
3	-OCH_3	85	84	85	82	90
4	-F	80	77	82	76	80
5	-Cl	70	65	70	63	75
6	-H	98, 96[c], 95[d]	95, 94[c], 92[d]	97	96	97
7	-C_2H_5	96	97	95	96	90
8	-OCH_3	92	89	90	92	95
9	-F	95	91	97	93	93
10	-Cl	75	80	82	81	93

[a]Conditions: 2 mol% catalyst; 4 h, 30ºC. [b]Yield was determined by GC. Isolated yield for [c]third run and [d]fifth run with reused catalyst.

Notably, catalytic reactions did not proceed at all in the absence of complexes; while the control experiments with metal salts ($Zn(NO_3)_2$ or $Cd(NO_3)_2$) did not show any trace of product. Furthermore, reaction immediately ceases when the catalyst is filtered off from the reaction. These experiments unambiguously confirm the catalytic role of complexes. Importantly, taking advantage of heterogeneous nature of reactions, all five complexes can be conveniently recovered by mere filtration after the completion of the reaction. Such recovered complexes can be reused without any purification or regeneration and were tested for five consecutive reactions without much loss of catalytic efficiency. The stability of all recovered complexes was analysed with X-ray powder diffraction (XRPD) studies and FTIR spectra. Both these studies showed identical results to that of freshly prepared samples (Figure S26-S28; ESI) and convincingly prove that the structural integrity of these complexes remain intact during the catalysis.

To understand the regioselectivity, styrene oxide was used as a representative asymmetrical substrate (entries 6 – 10; Table 1).[16b-e,] Importantly, a perfect regioselectivity was observed with a single product in all reactions.[16b-e] Out of two possible products due to the nucleophilic attack either at benzylic carbon or less hindered carbon atom of the epoxide; nucleophile exclusively attacked at the less hindered carbon atom. The regio-isomer showed the characteristic molecular ion peak at *m/z* [M^+-31] due to the loss of –CH_2OH fragment.[17a] Such an observation conclusively proves the formation of a single product as the other regio-isomer is expected to show the molecular ion peak [M^+ –107] due to the loss of C_6H_5CHOH fragment if the nucleophile had attacked the terminal carbon atom of the epoxide ring.[17a] Results suggest that the epoxide has approached the Lewis acidic metal through less hindered side assisted via the cavity structure.[18]

With the success of RORs, all five complexes were further tested for the CRs. CRs of carbonyl-based substrates offer a convenient route to cyanohydrins which are intermediates for a variety of fine chemicals and pharmaceuticals.[19] Extensive research has been devoted to develop improved Lewis acid catalysts for the reaction of cyanide ion with aldehydes.[20] In this context, heterogeneous catalysts incorporating Lewis acidic sites are advantageous.[16f,g] As displayed in Table 2, all five complexes were able to catalyse CRs of assorted aldehydes with trimethylsilylcyanide as the CN^- source. Benzaldehyde and several functionalized analogues provided the corresponding cyanohydrins in good to excellent yield. We propose that the catalysis is occurring via the displacement of labile nitrate

Dalton Transactions Accepted Manuscript

 This journal is © The Royal Society of Chemistry 2012

ions and/or MeOH molecules by aldehyde before its activation and reaction with cyanide. Importantly, all five complexes functioned as the heterogeneous catalysts whereas recyclability experiments substantiated that these complexes remain intact after the catalysis. Finally, no transformation was noted without catalysts while use of metal salt ($Zn(NO_3)_2$ or $Cd(NO_3)_2$) did not produce any cyanohydrin.

Table 2. Cyanation reactions of assorted aldehydes with $(CH_3)_3SiCN$ using complexes **1-5**.[a]

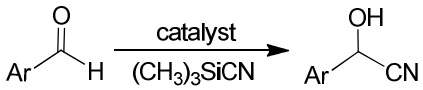

Entry	R	%Yield[b]				
		1	**2**	**3**	**4**	**5**
1	$-C_6H_5$	90,88[c],86[d]	95	95	96	96
2	3-MeOC_6H_4	97	95	96	93	95
3	4-MeOC_6H_4	94	93	94	95	93
4	$3\text{-NO}_2C_6H_4$	99	98	98	97	98
5	$4\text{-NO}_2C_6H_4$	90	97	91	97	89
6	4-ClC_6H_4	95	96	95	94	94
7	1-Naphthyl	98	90	97	96	90
8	2-Naphthyl	95	93	94	90	94
9	9-Anthryl	95	94	96	93	97

[a]Conditions: 5 mol% catalyst; 6 h, 30ºC. [b]Yield was determined by GC. Isolated yield for [c]third run and [d]fifth run with reused catalyst.

It is noteworthy to mention that the molecular size of the substrate and the electronic substituents present on substrates have negligible effect on the product yield. For example, CRs with sterically demanding aldehydes such as 1- and 2-naphthaldehyde as well as 9-anthraldehyde resulted in as good yield as noted for benzaldehyde. The results suggest that all aldehydic substrates have similar access

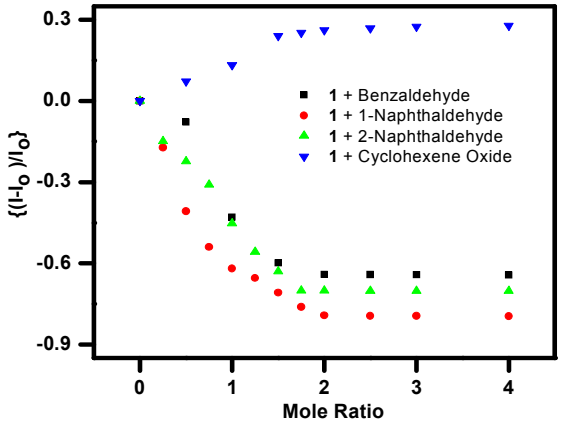

Figure 4. Plots of relative emission intensities versus amount of substrates (cyclohexene oxide ▼, benzaldehyde ■, 1-naphthaldehyde ●, and 2-naphthaldehyde ▲) in DMF-$CHCl_3$ (1:5).

and affinity to the Lewis acidic metal within the complex cavity. At this stage, we decided to confirm that the substrate(s) is indeed bound within the complex cavity. For such studies, complex **1** was used as a representative case which on excitation at 320 nm exhibited emission at ca. 460 nm. Importantly, when complex **1** was titrated with cyclohexene oxide, benzaldehyde and 1- and 2-naphthaldehyde; significant changes in the emission intensities were noted (Figure 4). While titration with cyclohexene oxide resulted in the enhancement of emission at ca. 460 nm (Figures S29-S31; ESI); similar titrations with benzaldehyde (Figure S32; ESI) as well as 1- and 2-naphthaldehyde caused considerable quenching in the emission intensities (Figures S33 – S37; ESI). It is worth to mention here that titrations using cyclohexene and naphthalene did not cause any change in the emission intensity, therefore, strongly suggesting that the complex cavity is specific for O-based substrates and such substrates are bound within the complex cavity and caused perturbation to the emission intensities.

The mole-ratio plot unambiguously showed a stoichiometry of 1:2 between complex **1** and substrates (cyclohexene oxide, 1- and 2-naphthaldehyde). A representative example of titration and fittings of complex **1** with 2-naphthaldehyde is shown in Figure 5. The results confirm that complex **1** binds two equivalents of substrates which were further proved by the Benesi-Hildebrand method.[21] The Benesi-Hildebrand equation is as follows:

$$1/[I - I_0] = 1/K(I_{max} - I_0)[\text{Substrate}]^n + 1/[I_{max} - I_0]$$

where I_0 is the emission intensity of complex **1**, I is the emission intensity obtained with substrate, I_{max} is the emission intensity obtained with excess amount of substrate, K is the association constant (M^{-2}), [substrate] is the concentration of substrate added (M), and n is the substrate equivalents. As shown in Figure 5, the plot of $1/(I - I_0)$ against $1/[\text{Substrate}]^2$ shows a liner relationship,

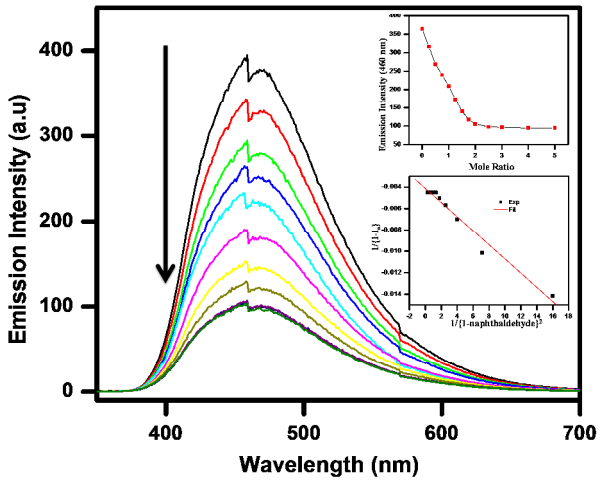

Figure 5. Fluorescence titration of complex **1** with 2-naphthaldehyde in DMF-$CHCl_3$ (1:5). Top inset: change in emission intensity as a function of moles of 2-naphthaldehyde. Bottom inset: Linear regression fitting curve for 1:2 binding between complex **1** and 2-naphthaldehyde.

indicating association with substrate in a 1:2 stoichiometry, therefore confirming the 1:2 stoichiometry.[22,23] The association constant, K, was determined from the slope. This method afforded the association constants (K x 10^5 M^{-2}) of 10.5, 9.8, and 9.0 for cyclohexene oxide, 1- and 2-naphthaldehyde, respectively. Notably, plots assuming stoichiometry of 1:1 as well as 1:3 do not show linear relationship of

Dalton Transactions Accepted Manuscript

$1/(I–I_0)$ against $1/[Substrate]^n$, therefore, ruling out both 1:1 and 1:3 but confirming a stoichiometry of 1:2 between complex and substrate. Importantly, these studies justify that a metal ion situated inside the cleft is able to bind all substrates with similar binding affinities. These experiments precisely prove our assumption that the catalysis starts after substrate coordinates to a metal center (Scheme S1, ESI).

We also attempted to understand if the binding of substrate within the complex cavity could also be evaluated by the FTIR spectral studies. Thus, when complex **1** was treated with a CH_2Cl_2 solution containing benzaldehyde, 1- or 2-naphthaldehyde and styrene oxide; noticeable spectral differences were observed when compared to neat samples. For example, $\nu_{C=O}$ stretch for the cavity bound benzaldehyde or 1/2-naphthaldehyde was red-shifted by ca. 15 cm^{-1}. More importantly, ν_{N-H} stretches of the complex cavity were also shifted implying that substrates are indeed bound within the complex cavity.

Oxidative catalytic applications

Notably, complex **5** contains Mn(II) ion and is coordinated by three labile MeOH molecules. Mn(II) ion is known to support oxidation reactions[23] and we selected oxidation of assorted olefins as epoxides constitute an important class of starting materials and intermediates.[24] Epoxidation reactions have been studied in detail; however, harsh reaction conditions and multiple oxidation products have limited wider commercial utilization.[25] We, therefore, targeted to use molecular oxygen as an oxidant in presence of isobutyraldehyde as a sacrificial oxidizing agent.[26] In order to optimize reaction conditions, styrene was selected as a model substrate. Thus, when a mixture of styrene (1 equiv.) and isobutyraldehyde (3 equiv.) was stirred with suspended complex **5** in MeCN under an oxygen atmosphere; a smooth reaction occurred to afford styrene oxide (92%) with a small amount of benzaldehyde (8%) as the by-product. Notably, oxidation reaction did not show any conversion in absence of complex **5** whereas use of THF or MeOH significantly affected the yield of styrene oxide. Further, solvent-free reaction conditions resulted in multiple products suggesting a cascade of oxidation reactions. We also attempted to understand the optimal loading of the catalyst in order to efficiently carry out the epoxidation reactions. For such a purpose, catalyst loading of 0.5, 1, 2, and 5 mol% were used for the oxidation of styrene. The product yield of styrene oxide varied in an anticipated manner in the following order: 0.5 (50) < 1 (60) < 2 (88) < 5 (92) and therefore we decided to use 4 mol% catalyst loading.

With these optimized reaction conditions; complex **5** showed catalytic oxidation of alkenes to epoxides within 4 h at room temperature (30 ºC). A variety of alkenes were tested; such as *para*-substituted styrenes (Table 3; entries 1-5); sterically bulkier alkenes (Table 3; entries 6-10); cyclic alkenes (Table 4; entries 1-5); and long-chain alkenes (Table 5; entries 1-4). For *para*-substituted styrenes, facile oxidation to epoxides resulted with aldehydes as the minor side product. Interestingly, for bulkier alkenes (entry 6-8), oxidation to epoxide decreases considerably with 9-vinylanthracene (entry 8) showing the minimum conversion. It appears that the approach of such substrates towards Mn(II) ion was significantly less-favoured due to the presence of hydrophobic vinyl group. It is important to mention that all aldehydic substrates caused quenching to the emission intensity of complex **1** and showed a stoichiometry of 1:2 suggesting that the complex cavity has affinity to bind O-based hydrophilic substrates. We, therefore, conclude that the hydrophilicity and not the size of a substrate control the catalysis outcome.

For the oxidation of *cis*- and *trans*-stilbene, stilbene oxide was the predominant product along with a small amount of benzaldehyde (entries 9-10). The oxidation of *cis*-stilbene was poor and afforded only 30% conversion while *trans*-stilbene was transformed in quantitative yield. We believe that *cis*- to *trans* isomerisation is one of the major factors for the observed stereo-selectivity; however, poor oxidation of *cis*-stilbene. Notably, only small amount of benzaldehyde was produced both in *cis*- and *trans*-stilbene epoxidation.

Table 3. Epoxidation of assorted olefins using complex **5**.[a]

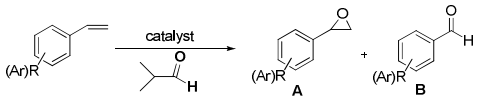

Entry	Ar / R	%Yield[b]		% Conversion
		A	**B**	
1	H	92[c], 90[d], 89[e]	8[c]	100
2	-OMe	90	8	98
3	-Me	92	8	100
4	-Cl	95	5	100
5	$-C(CH_3)_3$	78	18	96
6	1-vinylnaphthalene	55	11	66
7	2-vinylnaphthalene	60	12	72
8	9-vinylanthracene	54	12	66
9	*cis*-stilbene	26	4	30
10	*trans*-stilbene	92	8	100

[a]Conditions: 4 mol% catalyst; MeCN; 4 h, 30ºC. [b]Yield was determined by GC. [c]Isolated yield. [d]Second and [e]fourth run with reused catalyst.

Table 4. Epoxidation of cyclic olefins using complex **5**.[a]

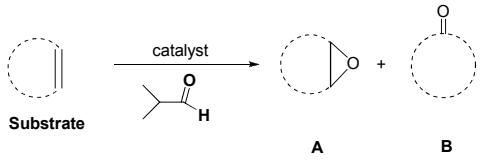

Entry	R	%Yield[b]		% Conversion
		A	**B**	
1		95	5	100
2		73	24[c]	97
3		74	25	99
4		74	26	100
5		100	0	100

[a]Conditions: 4 mol% catalyst; MeCN; 4 h; 30 ºC. [b]Yield was determined by GC. [c]Product is cyclohex-2-ene-1,4-dione.

Dalton Transactions Accepted Manuscript

This journal is © The Royal Society of Chemistry 2012

Complex **5** was also effective for the oxidation of cyclic alkenes (Table 4). In all cases, quantitative oxidation resulted, however, with variable proportions of products. Cyclopentene displayed the maximum amount of desired epoxide (95%) whereas higher ring analogues exhibited comparatively lower product yield (compare entries 1 – 4; Table 4). We speculate that higher ring analogues offered several structural conformations which caused undesirable oxidation of the ring. Interestingly, placement of methyl group adjacent to the double bond caused exclusive formation of epoxide with no sign of any by-product (entry 5). The oxidation of long-chain alkenes has been considered a difficult process and generally requires stronger oxidants.[21a] Noticeably, complex **5** effectively oxidizes such alkenes with 90 – 100% conversion (Table 5). Interestingly, conversion was quantitative in case of 1-hexene and 1-decene while other two alkenes afforded ca. 90% conversions. The reason for this behaviour is probably related to the optimal orientation of a substrate within the complex cavity in absence of other limiting parameters.

In order to ascertain the stability of complex **5** during the oxidative catalysis; catalyst **5** was recovered after the reaction and characterized. The FTIR spectrum of complex **5**, recorded after the catalysis, showed very similar spectral features as that of a pristine sample. Notably, however, one of the prominent features for the coordinated methanol molecule (O–C stretch at 1015 cm^{-1}) was in fact diminished whereas $\nu_{O\text{-}H}$ stretches were intensified. We, therefore, propose that the coordinated methanol molecules are first replaced by isobutyraldehyde and/or substrate molecules during the course of catalysis and subsequently by the water molecules after the catalysis. (Figure S16).

Table 5. Epoxidation of long-chain olefins using complex **5**.[a]

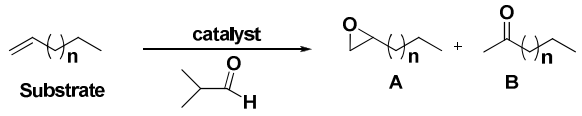

Entry	Substrate	%Yield[b]		% Conversion
		A	B	
1		74	26	100
2		73	18	91
3		78	15	93
4		98	2	100

[a]Conditions: 4 mol% catalyst; MeCN; 4 h; 30ºC. [b]Yield was determined by GC.

Experimental Section

General procedures

All reagents were purchased from the commercial sources and used without further purification. The solvents were dried and purified using standard procedures.[27]

Synthesis of H_2L^1. Pyridine-2,6-dicarboxylic acid (1.0 g, 0.0059 mol) and 2-aminothiazole (1.196g, 0.0119 mol) were taken in 25 ml pyridine and refluxed with stirring for 30 min at 120°C. $P(OPh)_3$ (3.877g, 0.0125 mol) was added drop-wise to the aforementioned reaction mixture. The reaction mixture was finally stirred at 70 °C for 12 h. The reaction mixture was poured to ice-cold water that caused precipitation of crude product which was filtered, washed with water followed by ethanol and dried. The crude product was recrystallized from MeOH/$CHCl_3$. Yield: 1.58 g (80 %). Anal. Calc. for $C_{13}H_9N_5O_2S_2$: C, 47.12; H, 2.74; N, 21.13; S, 19.35. Found: C, 47.52; H, 2.92; N, 20.83; S, 19.41. M.P.: 282-284 ºC. MS (ESI^+, $CHCl_3$, *m/z*): calcd. 331.0198 for H_2L^1; found 332.0291 for M + H^+; found 354.0110 for M + Na^+. FTIR spectrum (KBr pellet, cm^{-1}): 3109 (N-H), 1676 (C=O). ^{1}H NMR spectrum (400 MHz, $CDCl_3$): δ = 8.47 (d, *J*=8.1Hz, 2H), 8.18 (t, *J*=7.3Hz, 1H), 7.49 (d, *J*=3.6Hz, 2H), 7.03 (d, *J*=3.6Hz, 2H), 12.30 (broad, N-H). ^{13}C NMR spectrum (100 MHz, $CDCl_3$): 140.01 (C_1); 126.03 (C_2); 146.97 (C_3); 158.48 (C_4); 160.84 (C_5); 137.66 (C_6); 113.91 (C_7).

Synthesis of H_2L^2. This ligand was synthesized in a similar manner as mentioned for H_2L^1 with following reagents: pyridine-2,6-dicarboxylic acid (1.0 g, 0.0059 mol); 2-amino-2-thiazoline (1.222 g, 0.0119 mol); and $P(OPh)_3$ (3.877g, 0.0125 mol). The product was isolated after the removal of pyridine at reduced pressure followed by triturating the oily remains with methanol. Yield: 1.30 g (65%). Anal. Calc. for $C_{13}H_{13}N_5O_2S_2$: C, 46.55; H, 3.91; N, 20.88; S, 19.12. Found: C, 46.24; H, 4.21; N, 20.93; S, 19.25. M.P.: 220-222 ºC. MS (ESI^+, $CHCl_3$, *m/z*): calcd. 335.0511 for H_2L^2; found 336.0602 for M + H^+; found 358.0421 for M + Na^+. FTIR spectrum (KBr, cm^{-1}): 3219 (N-H), 1730, 1623 (C=O). ^{1}H NMR spectrum (400 MHz, $CDCl_3$): δ = 8.39 (d, *J*=8.1Hz, 2H), 8.11 (t, *J*=8.1Hz, 1H), 3.98 (t, *J*=8.1 Hz, 4H), 3.32 (t, *J*=8.1Hz, 4H), 11.07 (broad, N-H). ^{13}C NMR spectrum (100 MHz, $CDCl_3$): 139.80 (C_1); 126.27 (C_2); 147.12 (C_3); 158.74 (C_4); 161.91 (C_5); 56.58 (C_6); 33.35(C_7).

Synthesis of H_2L^3. This ligand was also prepared with a similar procedure with following chemicals: pyridine-2,6-dicarboxylic acid (1.0 g, 0.0059 mol); 2-aminobenzothiazole (1.792 g, 0.0119 mol), and $P(OPh)_3$ (3.877g, 0.0125 mol).. Recrystallization was achieved from THF. Yield: 1.95 g (76%). Anal. Calc. for $C_{21}H_{13}N_5O_2S_2$: C, 58.45; H, 3.04; N, 16.23; S, 14.86. Found: C, 58.62; H, 3.19; N, 15.95; S, 15.02. M.P.: 288-290 ºC. MS (ESI^+, $CHCl_3$, *m/z*): calcd. 431.0511 for H_2L^3; found 432.0602 for M + H^+; found 454.0422 for M + Na^+. FTIR spectrum (KBr, cm^{-1}): 3235 (N-H), 1695 (C=O). ^{1}H NMR spectrum (400 MHz, d_6-DMSO): δ = 13.60 (s, 1H), 8.48 (d, *J*=8.1Hz, 2H), 8.36 (t, *J*=8.1, 7.3Hz, 1H), 8.05 (d, *J*=16.1Hz, 2H), 7.88 (d, *J*=8.0Hz, 2H), 7.50 (d, *J*=8.1Hz, 2H), 7.36 (t, *J*=7.1Hz, 2H). ^{13}C NMR spectrum (100 MHz, $CDCl_3$): 140.52 (C_1); 124.11 (C_2); 147.37 (C_3); 158.11 (C_4); 162.92 (C_5); 131.75 (C_6); 121.96 (C_7); 126.43 (C_8); 127.07 (C_9); 120.78 (C_{10}); 148.71 (C_{11}).

Synthesis of [{$L^1(H)_2$}$Zn(NO_3)_2$] (1). Ligand H_2L^1 (0.2 g, 0.604 mmol) was dissolved in 5 mL $CHCl_3$ and layered with a solution of $[Zn(H_2O)_6](NO_3)_2$ (0.179 g, 0.604 mmol) dissolved in 3 mL MeOH. White crystalline compound appeared within a day. Yield: 0.114 g (71%). Anal. Calc. for $C_{13}H_9ZnN_7O_8S_2$: C, 29.98; H, 1.74; N, 18.83; S, 12.31. Found: C, 29.64; H, 1.51; N, 18.34; S, 12.08. FTIR spectrum (Zn-Se ATR, cm^{-1}): 3276 (N-H), 1637 (C=O), 1345, 1282, 1016 (N-O). Molar conductivity (DMF ~ 1mM solution, 298 K): Λ_M = 140 Ω^{-1} cm^2 mol^{-1} (the range for 1:2 electrolyte in DMF is 130 - 170). Molar conductivity (DMSO ~ 1mM solution, 298 K): Λ_M = 90 Ω^{-1} cm^2 mol^{-1}. ^{1}H NMR spectrum (400 MHz, d_6-DMSO): δ = 13.37 (s, 2H), 8.45 (d, *J*=8.1Hz, 2H), 8.35 (dd, *J*=7.3-8.1Hz, 1H), 7.66 (d, *J*=3.7Hz, 2H), 7.40 (d, *J*=2.3Hz, 2H).

Synthesis of [{$L^1(H)_2Cd(NO_3)_2$}$_2$(μ-CH_3OH)] (2). Complex **2** was synthesised in a similar manner as that of complex **1** by using following reagents: H_2L^1 (0.2 g, 0.604 mmol) and $[Cd(H_2O)_6](NO_3)_2$ (0.175 g, 0.604

Dalton Transactions Accepted Manuscript

mmol). Yield: 0.125 g (73%). Anal. Calc. for $C_{27}H_{22}Cd_2N_{14}O_{17}S_4$: Calc: C, 27.77; H, 1.90; N, 16.79; S, 10.98. Found: C, 27.60; H, 1.96; N, 16.64; S, 10.62. FTIR spectrum (Zn-Se ATR, cm^{-1}): 3195 (N-H), 1619 (C=O), 1355, 1274, 1027 (N-O). Molar conductivity (DMF ~ 1mM solution, 298 K): Λ_M = 150 Ω^{-1} cm^2 mol^{-1} (the range for 1:2 electrolyte in DMF is 130 - 170). Molar conductivity (DMSO ~ 1mM solution, 298 K): Λ_M = 100 Ω^{-1} cm^2 mol^{-1}. ^{1}H NMR spectrum (400MHz, d_6-DMSO): δ = 13.39 (s, 2H), 8.44 (d, *J*=8.1Hz, 2H), 8.38(dd, *J*= 7.2-8.2Hz, 1H), 7.66 (d, *J*=3.7Hz, 2H), 7.40 (d, *J*=3.7Hz, 2H).

Synthesis of [{L^2(H)$_2$}Zn(NO$_3$)$_2$] (3). Complex **3** was synthesised in a similar manner as mentioned for complex **1** using the following reagents: H_2L^2 (0.2 g, 0.593 mmol) and $[Zn(H_2O)_6](NO_3)_2$ (0.173 g, 0.593 mmol). Yield 0.115 g (74%). Anal. Calc. for $C_{13}H_{13}ZnN_7O_8S_2.CH_3OH.H_2O$: C, 29.25; H, 3.30; N, 17.06; S, 11.16. Found: C, 29.11; H, 3.44; N, 17.18; S, 11.32. FTIR spectrum (Zn-Se ATR, cm^{-1}): 3323 (N-H), 1654 (C=O), 1346, 1287, 1018 (N-O). Molar conductivity (DMF ~ 1mM solution, 298 K): Λ_M = 145 Ω^{-1} cm^2 mol^{-1} (the range for 1:2 electrolyte in DMF is 130 - 170). Molar conductivity (DMSO ~ 1mM solution, 298 K): Λ_M = 95 Ω^{-1} cm^2 mol^{-1}. ^{1}H NMR spectrum (400 MHz, d_6-DMSO): δ = 10.11 (broad, 2H), 8.15-8.69 (broad, 3H), 3.58-4.15 (broad, 8H).

Synthesis of [{L^2(H)$_2$}Cd(NO$_3$)$_2$] (4). Ligand H_2L^2 (0.2 g, 0.593 mmol) dissolved in 5 mL DMA was layered by a solution of $[Cd(H_2O)_6](NO_3)_2$ (0.173 g, 0.593 mmol) dissolved in 8 mL MeOH. This solution was left for evaporation at room temperature. White crystalline product appeared within 48 h. Yield: 0.116 g (69%). Anal. Calc. for $C_{13}H_{13}CdN_7O_8S_2$: C, 27.25; H, 1.60; N, 17.27; S, 11.29. Found: C, 26.97; H, 1.68; N, 17.13; S, 11.13. FTIR spectrum (Zn-Se ATR, cm^{-1}): 3319 (N-H), 1637 (C=O), 1335, 1268, 1026 (N-O). Conductivity (DMF ~ 1mM solution, 298 K): Λ_M = 143 Ω^{-1} cm^2 mol^{-1} (the range for 1:2 electrolyte in DMF is 130 - 170). Molar conductivity (DMSO ~ 1mM solution, 298 K): Λ_M = 92 Ω^{-1} cm^2 mol^{-1}. ^{1}H NMR spectrum (400 MHz, d_6-DMSO): δ = 10.42 (broad, 2H), 8.26-8.72 (broad, 3H), 3.71-4.02 (broad, 8H).

Synthesis of [MnL^3](CH$_3$OH)$_3$ (5). Ligand H_2L^3 (0.1 g, 0.232 mmol) was dissolved in N_2 flushed DMF (5 mL) and treated with NaH (0.012g, 0.487 mmol). The resulting solution was stirred for 10 min at room temperature followed by the drop-wise addition of a solution of $[Mn(H_2O)_6](ClO_4)_2$ (0.083g, 0.232 mmol) dissolved in 3 mL DMF. The reaction mixture was stirred for 1 h. The solvent was removed under reduced pressure and the oily remains were treated with CH_3CN to afford a yellow solid. Crude compound thus obtained was washed with diethyl ether and dried. This product was dissolved in DMF, passed through a pad of celite and the filtrate was layered with MeOH to afford yellow crystalline product within a day. Yield: 0.09 g (67 %). Anal. Calc. for $C_{24}H_{23}MnN_5O_5S_2$: C, 49.65; H, 3.99; N, 12.06; S, 11.05. Found: C, 49.32; H, 4.21; N, 11.52; S, 10.65. FTIR (Zn-Se ATR, cm^{-1}): 3455 (OH), 1612 (C=O), 1016 (O-CH_3).

General Procedure for Catalytic Reaction: For aminolysis, 1 equiv. of epoxide was treated with 1.1 equiv. of aniline or substituted aniline in presence of 2 mol% catalyst. In a typical cyanation reaction, 5 mol% catalyst was added to a mixture of aldehyde (1 equiv.) and trimethylsilylcyanide (5 equiv.). For both these reaction, the mixture was stirred at ambient conditions for 4 – 6 h. For epoxidation reactions, alkenes (1 equiv.) were treated with isobutyraldehyde (3 equiv.) in presence of 4 mol% catalyst **5** in MeCN under an oxygen atmosphere for 4 h. In all cases, reactions were monitored by thin-layer chromatography (TLC) and/or gas chromatography (GC). After mentioned time, catalyst was filtered off and the filtrate was concentrated under reduced pressure. The crude product was purified using flash column chromatography on silica gel using hexanes/ethyl acetate mixture (5:1) as the eluent. The products were separated, isolated and analyzed by GC and/or GC-MS techniques. The recovered catalysts were washed with diethyl ether, dried and reused without further purification or regeneration. Moreover, the recovered catalysts were characterized by FTIR spectra as well as by the X-ray powder diffraction studies. Both these studies showed identical results to those of the pristine samples.

Physical Measurements. The conductivity measurements were carried out with a digital conductivity bridge from the Popular Traders, India (model number: PT 825). The elemental analysis data were obtained with an Elementar Analysen Systeme GmbH Vario EL-III instrument. The NMR spectral measurements were carried out with a Jeol 400 MHz instrument. The FTIR spectra (Zn-Se ATR) were recorded with a Perkin–Elmer Spectrum–Two spectrometer. The absorption spectra were recorded with a Perkin–Elmer Lambda 25 spectrophotometer. GC and GC–MS studies were performed with a Perkin Elmer Clarus 580 and Shimadzu QP 2010 instrument, respectively, with RTX-5SIL-MS column. The X-ray powder diffraction studies were performed either with an X'Pert Pro from Panalytical or a Bruker AXS D8 Discover instrument (Cu-*K*α radiation, λ = 1.54184 Å). The samples were ground and subjected to the range of θ = 2–50° with a scan rate of 1° per minute at room temperature.

Crystallography. The intensity data were obtained with a Bruker Kappa Apex-CCD and Oxford XCalibur CCD diffractometer for complexes **1**-**4** and **5**, respectively, by using graphite-monochromated Mo-*K*α radiation (λ = 0.71073 Å).[28,29] For complexes **1** – **4**, intensity data were corrected for Lorentz polarization effects while an empirical absorption correction (SADABS) was applied.[30,31] A multi-scan absorption correction was applied using CrysalisPRO for complex **5**.[29] The structures were solved by the direct methods using SIR-92[32] and refined by full-matrix least-squares refinement techniques on F^2 using SHELXL97.[33] The hydrogen atoms were placed into the calculated positions and included in the last cycles of the refinement. All calculations were done using WinGX software package.[34] The refinement of complex **2** showed that the asymmetric unit contains two nitrate ions, both of them were disordered. For the first one (with atoms N6, O3, O4, and O5); disorder could only be resolved for O5. The second nitrate ion (with atoms N7, O6, O7, and O8) when refined with site occupancy factor (SOF) 1.00 gave high Ueq values. Thus, these atoms were subsequently refined with SOF of 0.5 which improved their Ueq values significantly. Both nitrate ions were refined with restraints over their bond lengths. There was a disordered methoxide ion sitting on the centre of inversion and bridging two monomeric halves. This methoxide ion was refined by keeping carbon atom on the centre of inversion with its SOF as 0.5 and two oxygen atoms (appearing in the Fourier) as the disordered oxygen atoms of the methoxide ion. These atoms were refined with part instruction with their SOF and thermal parameters being refined as free variables. Their combined SOF was refined to be equal to 0.5, so that there is half molecule of methoxide ion in the asymmetric unit. The disorder of methoxide oxygen atom could be successfully resolved and it was refined anisotropically as well. However, hydrogen atoms of methoxide ion could not be located. The final difference Fourier shows some electron density around the methoxide ion and also around the metal ion. The latter may be due to the series termination error. The hydrogen atoms attached to nitrogen atoms of the thiazole rings were easily located from the difference Fourier and were included with fixed N-H distances (0.88 Å) and Uiso 1.2 times that of the corresponding nitrogen atoms. For complex **5**, disordered oxygen atom (O4) was resolved by fixing it at two positions using part command. Details of the crystallographic data collection and structural solution parameter are provided in Table S8. CCDC- 1011221-1011225

Dalton Transactions Accepted Manuscript

This journal is © The Royal Society of Chemistry 2012

contain the supplementary crystallographic data for this paper. These data can be obtained free of charge from The Cambridge Data Center via www.ccdc.cam.ac.uk/data_request/cif.

Conclusions

This work has shown the synthesis and characterization of a few mononuclear coordination complexes with amide-based ligands containing appended heterocyclic rings. Interestingly, metal complexes displayed the migration of amidic N-H protons to the appended heterocyclic rings during the synthesis. Such protonated heterocyclic rings create a hydrogen bond based cavity adjacent to metal ion and assist in binding of O-based substrates within the complex cavity. The binding studies confirm that the substrates are bound within the complex cavity closer to the Lewis acidic metal in complexes **1** – **5** and oxidation-sensitive Mn ion in complex **5**. All complexes have been utilized as the reusable and heterogeneous catalysts for the ring-opening reactions of assorted epoxides; cyanation reactions of various aldehydes; and epoxidation reactions of several olefins. The work presented in this manuscript illustrates a viable method of designing substrate-specific cavity reminiscent to biological catalysts.

Acknowledgements

RG acknowledges Council of Scientific and Industrial Research (CSIR) and the University of Delhi for the financial support. Authors thank the CIF-USIC at this university for the instrumental facilities and crystallographic data collection. DB thanks UGC for a SRF fellowship.

Notes and references

[a] Department of Chemistry, University of Delhi, Delhi-110007. Phone: +91-11-27666646. Email: rgupta@chemistry.du.ac.in.
[b] Guru Nanak Dev University, Amritsar, Punjab – 143005.

Electronic Supplementary Information (ESI) available: [Figures for absorption, NMR, FTIR, mass, emission spectra, binding curves, and crystal structures; and tables for bonding parameters, weak interactions, and data collection]. See DOI: 10.1039/b000000x/

†The structure solution of complex **2** offered two crystallographic possibilities. First in which two monomeric halves are bridged by a methanol molecule while all coordinated nitrate ions have full site occupancy. Second; where two monomeric halves are bridged by a methoxide ion while two and one nitrate ions are respectively modelled with full and half site occupancy. Although the latter model converged better but our analytical data support the former formulation.

1. (a) R. Yamaguchi, K. Fujita, *Ligand Platforms in Homogenous Catalytic Reactions with Metals: Practice and Applications for Green Organic Transformations*, (2014) Wiley; (b) A. J. L. Pombeiro, Ed. *Advances in Organometallic Chemistry* (2013), Wiley.
2. (a) D. Natale and J. C. Mareque-Rivas, *Chem. Commun.*, 2008, 425; (b) R. L. Shook and A. S. Borovik, *Chem. Commun.*, 2008, 6095; (c) L. Brammer, Dalton Trans., 2003, 3145.
3. (a) D. W. Christianson and J. D. Cox, *Annu. Rev. Biochem.*, 1999, **68**, 33; (b) I. Schlichting, J. Berendzen, K. Chu, A. M. Stock, S. A. Maves, D. E. Benson, R. M. Sweet, D. Ringe, G. A. Petsko and S. G. Sligar, *Science*, 2000, **287**, 1615; (c) N. Yamamoto, S. Danos, P. D. Bonnitcha, T. W. Failes, E. J. New and T. W. Hambley, *J. Biol. Inorg. Chem.*, 2008, **13**, 861.
4. (a) Y. Lu and J. S. Valentine, *Curr. Opin. Struct. Biol.*, 1997, **7**, 495; (b) J. H. Dawson, *Science*, 1988, **240**, 433; (c) P. R. O. De Montellano, *Acc. Chem. Res.*, 1987, **20**, 289.
5. (a) A. S. Borovik, *Acc. Chem. Res.*, 2005, **38**, 54; (b) L. M. Berreau, *Eur. J. Inorg. Chem.* 2006, 273; (c) A. Wada, S. Yamaguchi, K. Jitsukawa, and H. Masuda, *Angew. Chem. Int. Ed.* 2005, **44**, 5698; (d) J. C. Mareque-Rivas and R. Prabaharan, *Chem. Commun.* 2004, 76.
6. (a) P. J. Donoghue, A. K. Gupta, D. W. Boyce, C. J. Cramer, and W. B. Tolman, *J. Am. Chem. Soc.* 2010, **132**, 15869; (b) P. J. Donoghue, J. Tehranchi, C. J. Cramer, R. Sarangi, E. I. Solomon, and W. B. Tolman, *J. Am. Chem. Soc.* 2011, **133**, 17602; (c) M. R. Halvagar, B. Neisen, and W. B. Tolman, *Inorg. Chem.* 2013, **52**, 793; (d) M. R. Halvagar and W. B. Tolman, *Inorg. Chem.* 2013, **52**, 8306; (e) J. Tehranchi, P. J. Donoghue, C. J. Cramer, and W. B. Tolman, *Eur. J. Inorg. Chem.* 2013, 4077.
7. (a) D. Huang and R. H. Holm, *J. Am. Chem. Soc.* 2010, **132**, 4693; (b) D. Huang, O. V. Makhlynets, L. L. Tan, S. C. Lee, E. V. Rybak-Akimova, and R. H. Holm, *Proc. Nat. Acad. Sci.* 2011, **108**, 1222; (c) D. Huang, O. V. Makhlynets, L. L. Tan, S. C. Lee, E. V. Rybak-Akimova, and R. H. Holm, *Inorg. Chem.* 2011, **50**, 10070; (d) X. Zhang, D. Huang, Y-S. Chen, and R. H. Holm, *Inorg. Chem.* 2012, **51**, 11017.
8. (a) A. Rajput and R. Mukherjee, *Coord. Chem. Rev.* 2013, **257**, 350; (b) H. L. Kwong, H. L. Yeung, C. T. Yeung, W. S. Lee, C. S. Lee and W. L. Wong, *Coord. Chem. Rev.* 2007, **251**, 2188; (c) O. Belda and C. Moberg, *Coord. Chem. Rev.* 2005, **249**, 727; (d) D. S. Marlin and P. K. Mascharak, *Chem. Soc. Rev.* 2000, **29**, 69.
9. D. Wang, S. V. Lindeman, and A. T. Fiedler, *Eur. J. Inorg. Chem.* 2013, 4473.
10. S. M. Redmore, C. E. F. Rickard, S. J. Webb, and L. J. Wright, *Inorg. Chem.* 1997, **36**, 4743.
11. K. Nakamoto, *Infrared and Raman Spectra of Inorganic and Coordination Compounds*, John Wiley & Sons, New York, **1986**.
12. W. J. Geary, *Coord. Chem. Rev.* 1971, **7**, 81.
13. A. W. Addition, T. N. Rao, J. Reedjik, J. Van Rinj, and G. C. Verschoor, *J. Chem. Soc. Dalton Trans.* 1984, 1349.
14. (a) W. Holderich, U. Barsnick, in *Fine Chemicals Through Heterogeneous Catalysis*, Ed. R. A. Sheldon, H. van Bekkum, 2001, Wiley-VCH, Weinheim. (b) C. J. Morten, A. J. Byers, A. R. Van Dyke, I. Vilotijevic, and T. F. Jamison, *Chem. Soc. Rev.* 2009, **38**, 3175. (c) K. B. Sharpless and T. R. Verhoeven, *Aldrichim. Acta* 1979, **12**, 63.
15. (a) J. Yamada, M. Yumoto, and Y. Yamamoto, *Tetrahedron Lett.* 1989, **30**, 4255; (b) S. Sagawa, H. Abe, Y. Hase, and T. Inaba, *J. Org. Chem.* 1999, **64**, 4962; (c) J. Auge and F. Leroy, *Tetrahedron Lett.* 1996, **37**, 7715; (d) M. Chini, P. Croti, L. Favero, M. Macchia, and M. Pineschi, *Tetrahedron Lett.* 1994, **35**, 433; (e) T. Ollevier and G. Lavie-Compin, *Tetrahedron Lett.*

Dalton Transactions Accepted Manuscript

2004, **45**, 49; (f) L. R. Reddy, M. A. Reddy, N. Bhanumati, and K. R. Rao, *Synthesis* 2001, 831. (g) A. K. Chakraborti and A. Kondaskar, *Tetrahedron Lett.* 2003, **44**, 8315; (h) P. Q. Zhao, L. W. Xu, and C. G. Xia, *Synlett.* 2004, 846; (i) A. Kamal, R. Ramu, M. A. Azhar, and G. B. R. Khanna, *Tetrahedron Lett.* 2005, **46**, 2675.

16. (a) A. Mishra, A. Ali, S. Upreti, and R. Gupta, *Inorg. Chem.* 2008, **47**, 154; (b) A. Mishra, A. Ali, S. Upreti, M. S. Whittingham and R. Gupta, *Inorg. Chem.,* 2009, **48**, 5234; (c) G. Kumar, A. P. Singh, and R. Gupta, *Eur. J. Inorg. Chem.* 2010, 5103; (d) A. P. Singh, A. Ali, and R. Gupta, *Dalton Trans.* 2010, **39**, 8135; (e) A. P. Singh, G. Kumar, and R. Gupta, *Dalton Trans.* 2011, **40**, 12454; (f) G. Kumar and R. Gupta, *Inorg. Chem.* 2012, **51**, 5497; (g) G. Kumar and R. Gupta, *Inorg. Chem.* 2013, **52**, 10773.
17. (a) B. Shivani, Pujala, and A. K. Chakraborti, *J. Org. Chem.* 2007, **72**, 3713. (b) G. Mancilla, M. Femenia-Rios, J. Macias-Sanchez, and I. G. Collado, *Tetrahedron*, 2008, **64**, 11732.
18. It may, however, be noted that the benzylic position is susceptible to nucleophilic attack due to the electronic effect of phenyl ring; see ref. 17a.
19. (a) U. Muller, M. M. Schubert, O. M. Yaghi, *Handbook of Heterogeneous Catalysis;* Ed. G. Ertl, H. Knozinger, F. Schuth, J. Weitkamp, Wiley-VCH: Weinheim, Germany, 2008. (b) R. J. H. Gregory, *Chem. Rev.* 1999, **99**, 3649. (c) M. North, *Tetrahedron: Asymmetry* 2003, **14**, 147. (d) J. M. Brunel and I. P. Holmes, *Angew. Chem., Int. Ed.* 2004, **43**, 2752.
20. (a) D. H. Ryu and E. J. Corey, *J. Am. Chem. Soc.* 2004, **126**, 8106. (b) J. M. Keith and E. N. Jacobsen, *Org. Lett.* 2004, **6**, 153. (c) Y. Hamashima, D. Sawada, M. Kanai, and M. Shibasaki, *J. Am. Chem. Soc.* 1999, **121**, 2641. (d) Y. Hamashima, M. Kanai, and M. Shibasaki, *Tetrahedron Lett.* 2001, **42**, 691. (e) S. Masumoto, K. Yabu, M. Kanai, and M. Shibasaki, *Tetrahedron Lett.* 2002, **43**, 2919. (f) Y. Hamashima, M. Kanai, and M. Shibasaki, *J. Am. Chem. Soc.* 2000, **122**, 7412. (g) C. Baleizao, B. Gigante, H. Garcia, and A. Corma, *Tetrahedron Lett.* 2003, **44**, 6813. (h) C. Baleizao, B. Gigante, H. Garcia, and A. Corma, *Green Chem.* 2002, **4**, 272. (i) M. Mori, and H. Imma, T. Nakai, *Tetrahedron Lett.* 1997, **38**, 6229.
21. H. A. Benesi and J. H. Hildebrand, *J. Am. Chem. Soc.* 1949, **71**, 2703.
22. (a) Y. Shiraishi, S. Sumiya, Y. Kohno, and T. Hirai, *J. Org. Chem.* 2008, **73**, 8571. (b) S. Srivastava, A. Ali, A. Tyagi, and R. Gupta, *Eur. J. Inorg. Chem.* 2014, 2113.
23. (a) R. A. Sheldon and J. K. Kochi, *Metal Catalyzed Oxidation of Organic Compounds*, Academic Press, New York, 1981; (b) P. Gamez, P. G. Aubel, W. L. Driessen, and J. Reedjik, *Chem. Soc. Rev.* 2001, **30**, 376; c) B. Meunier, *Biomimetic Oxidations Catalyzed by Transition Metal Complexes*, Imperial College Press, London, 2000.
24. (a) S. Y. Ko, A. W. M. Lee, S. Masamune, L. A. Reed, K. B. Sharpless, and F. J. Walker, *Science* 1983, **220**, 949; (b) K. C. Nicolaou, N. Winssinger, J. Pastor, S. Ninkovic, F. Sarabia, Y. He, D. Vourloumis, Z. Yang, T. Li, P. Giannakakou, and E. Hamel, *Nature* 1997, **387**, 268; (c) D. J. Darensbourg, R. M. Mackiewicz, A. L. Phelps, and D. R. Billodeaux, *Acc. Chem. Res.* 2004, **37**, 836; (d) E. N. Jacobsen, *Catalytic Asymmetric Synthesis* (Ed.: I. Ojima), VCH Publishers, New York, 1993, p. 229; (e) G. De Faveri, G. Ilyashenko, and M. Watkinson, *Chem. Soc. Rev.* 2011, **40**, 1722.
25. (a) K.-P. Ho, W.-L. Wong, K.-M. Lam, C.-P. Lai, T. H. Chan, and K.-Y. Wong, *Chem. Eur. J.* 2008, **14**, 7988; (b) S. Groni, P. Dorlet, G. Blain, S. Bourcier, R. Guillot, and E. Anxolabéhère-Mallart, *Inorg. Chem.* 2008, **47**, 3166; (c) G. Yin, A. M. Danby, D. Kitko, J. D. Carter, W. M. Scheper, and D. H. Busch, *Inorg. Chem.* 2007, **46**, 2173.
26. J. Singh, G. Hundal, and R. Gupta, *Eur. J. Inorg. Chem.* 2008, 2052.
27. D. D. Perrin, W. L. F. Armarego, and D. R. Perrin, *Purification of Laboratory Chemicals*, Pergamon Press, Oxford, 1980.
28. SMART: Bruker Molecular Analysis Research Tool, version 5.618, Bruker Analytical X-ray System, 2000.
29. CrysAlisPro, Oxford Diffraction Ltd., version 1.171.33.49b (2009).
30. SAINT-NT, Version 6.04, Bruker Analytical X-ray System, 2001.
31. SHELXTL-NT, Version 6.10, Bruker Analytical X-ray System, 2000.
32. A. Altomare, G. Cascarano, C. Giacovazzo, A. Guagliardi, *J. Appl. Crystallogr.* 1993, **26**, 343.
33. G. M. Sheldrick, *Acta Cryst.* 2008, **A64**, 112.
34. L. J. Farrugia, WinGX version 1.64, An Integrated System of Windows Programs for the Solution, Refinement and Analysis of Single-Crystal X-ray Diffraction Data; Department of Chemistry, University of Glasgow, 2003.

Dalton Transactions Accepted Manuscript

 This journal is © The Royal Society of Chemistry 2012